

D-Band Flip-Chip Packaging with Wafer-Level Cu-pillar Bumps

1st Zhibo Cao
IHP – Leibniz-Institut für innovative
Mikroelektronik
Frankfurt Oder, Germany
cao@ihp-microelectronics.com

4th Jens Lehmann
IHP – Leibniz-Institut für innovative
Mikroelektronik
Frankfurt Oder, Germany
lehmann@ihp-microelectronics.com

7th Matthias Wietstruck
IHP – Leibniz-Institut für innovative
Mikroelektronik
Frankfurt Oder, Germany
wietstruck@ihp-microelectronics.com

2nd Matteo Stocchi
Keysight Technologies
Böblingen, Germany
matteo.stocchi1988@gmail.com

5th Lei Li
ECE Department
Cornell University
Ithaca, USA
ll886@cornell.edu

8th Corrado Carta
Technische Universität Berlin
IHP – Leibniz-Institut für innovative
Mikroelektronik
Frankfurt Oder, Germany
carta@ihp-microelectronics.com

3rd Christian Wipf
IHP – Leibniz-Institut für innovative
Mikroelektronik
Frankfurt Oder, Germany
wipf@ihp-microelectronics.com

6th Selin Tolunay Wipf
IHP – Leibniz-Institut für innovative
Mikroelektronik
Frankfurt Oder, Germany
tolunay@ihp-microelectronics.com

9th Mehmet Kaynak
Kilby Lab, Texas Instrument
Dallas, USA
kaynakmehmet@icloud.com

Abstract— The transmission loss of a Cu pillar microstrip-microstrip transition in a flip-chip package is characterized. The used components are fabricated in the back-end layers of a standard BiCMOS process, with Cu pillars deposited on top as the flipped die and UBM coating on pad as the substrate. Four variations with different pitches and openings on the ground plane are all characterized and compared using both measurement and FEM simulation. It is found that a small pitch with a de-coupling aperture on the ground plane are the keys to minimize the transition losses. The de-embedded insertion loss of a single Cu-pillar transition is between 0.3-0.5 dB over 110-170 GHz (D-band). Such a wafer-level bumping approach greatly improves the throughput and uniformity, and meanwhile, demonstrates comparable transition losses with other flip-chip packages using similar sized bumps.

Keywords—Cu pillar, flip-chip, D-band, microstrip, FEM

I. INTRODUCTION

As the transistors approach their physical limits, the research focus starts to shift to the heterogeneous integration towards “More than Moore” technologies. The package solutions for mm-wave applications is, of course, an important aspect to be considered.

The conventional wire bond, although is still under development, is limited by its bandwidth due to the large wire inductance [1][2]. The flip-chip packaging and the fan-out wafer level packaging have both demonstrated outstanding RF capabilities [3-6]. In this study, a Cu pillar bumped flip-chip package is developed and characterized. The advantage of this approach is its small pitch, small bump sizes, and its uniformity as a wafer-level bumping process. All these features are critically advantageous in the mm-wave range, making it a promising packaging solution for applications at D-band and above.

II. METHODOLOGY

A. Sample design

Since the targeted band is 110-170 GHz, the substrates used in the flip-chip assembly should be carefully selected to

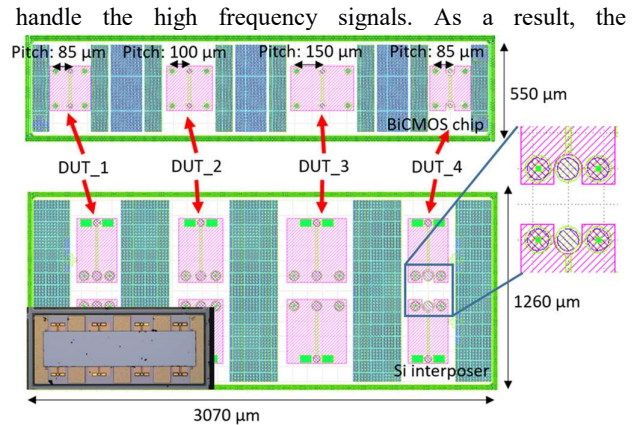


Fig. 1 The flip-chip samples, both the GDS layout and the fabricated test vehicles are shown. There are four variations with different pitches and de-coupling apertures on the ground.

handle the high frequency signals. As a result, the transmission lines are designed in the standard BiCMOS back-end stacks using IHP’s state-of-the-art SG13 BEOL runs. Two dies are flip-chip assembled, one smaller die is used to accommodate Cu pillars, and the other larger die is used as substrate with under-bump-metallization (UBM) coatings on the pads. As is shown in Fig. 1, a microstrip-to-microstrip transition structure is exploited, with four variations for comparison. The first three variations differ in pitch, which ranges from 85 μm to 150 μm , and the last one uses a de-coupling aperture on the ground plane to minimize the parasitic capacitances.

Since the pillars have around 15 μm of SnAg solder cap on top, the flip-chip assembly is implemented using a mass solder reflow process. The die with pillars is first dipped in a tray with flux materials, then flipped and aligned with the Fineplacer Pico bonder. The assembled chips are cleaned with ultra-sonic after the reflow to remove the excessive flux materials and ensure low losses in the D-band.

To enable a direct evaluation of the influences of the Cu pillar transitions, the structure is compared with a plain

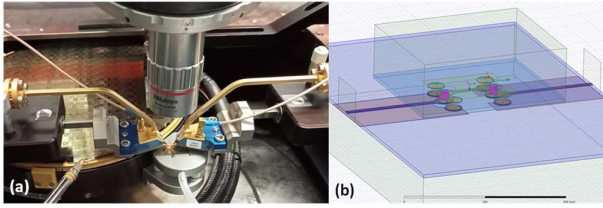


Fig. 2 The measurement and simulation setups. (a) is the D-band on wafer measurement setup, and (b) is the HFSS simulation setup.

microstrip line. With such objective, several microstrips with different lengths are designed and fabricated using the same technology.

B. Simulation setup

The modelling of the Cu pillar transition is implemented in Ansoft HFSS. Such a full-wave solver ensures the accuracy of the modelling, which is especially critical for complex 3D structures working at such high frequencies. The model is fully parametrized to ease the study of different geometry variations. The details of the modelling are illustrated below.

The driven modal is utilized to solve for the S parameters. And considering the wide bandwidth (110 GHz to 170 GHz), discrete solutions are needed to ensure the modelling accuracy over the whole frequency band. Besides, wave ports are directly used on the transmission line without pads to be comparable with de-embedded measurement results. A radiation boundary is assigned in order to minimize the reflected waves. The HFSS model is shown in Fig. 2, together with the measurement setup discussed below.

C. Measurement

The measurement setup is shown in Fig. 3. Rhode & Schwarz ZVA 24 is used together with frequency extenders to measure from 110 GHz to 170 GHz. Since the packaged sample is too small to be fixed on the wafer chuck, it is placed on an auxiliary chuck. Infinity probes with a pitch of 75 μm are used.

Worth noticing that the probe contact is problematic to the UBM coating. The few-micrometer-thick Nickel is too hard for the probes to penetrate, leading to small contact areas. This results in a contact resistance ranging from a few Ohms to tens of Ohms depending on the contact attempt. Two indicators are taken to measure the quality of the contact: 1) the VNA frequency sweeping results should be stable over time, and 2) the S11 and S22 should be similar due to the symmetry of the structures. With these considerations, proper contacts are ensured.

However, even with a proper contact, the contact resistance is still much higher than that on the aluminum pads. To make sure the obtained results are comparable with those in the literature, de-embedding is necessary. A TRL method, which is suitable for the D-band frequencies, is employed for all the measurements to remove the pad effects since all the pad configurations are the same.

III. RESULTS AND DISCUSSION

The comparisons of measurement and simulation for all four flip-chip structures are shown in Fig. 3. Good matchings

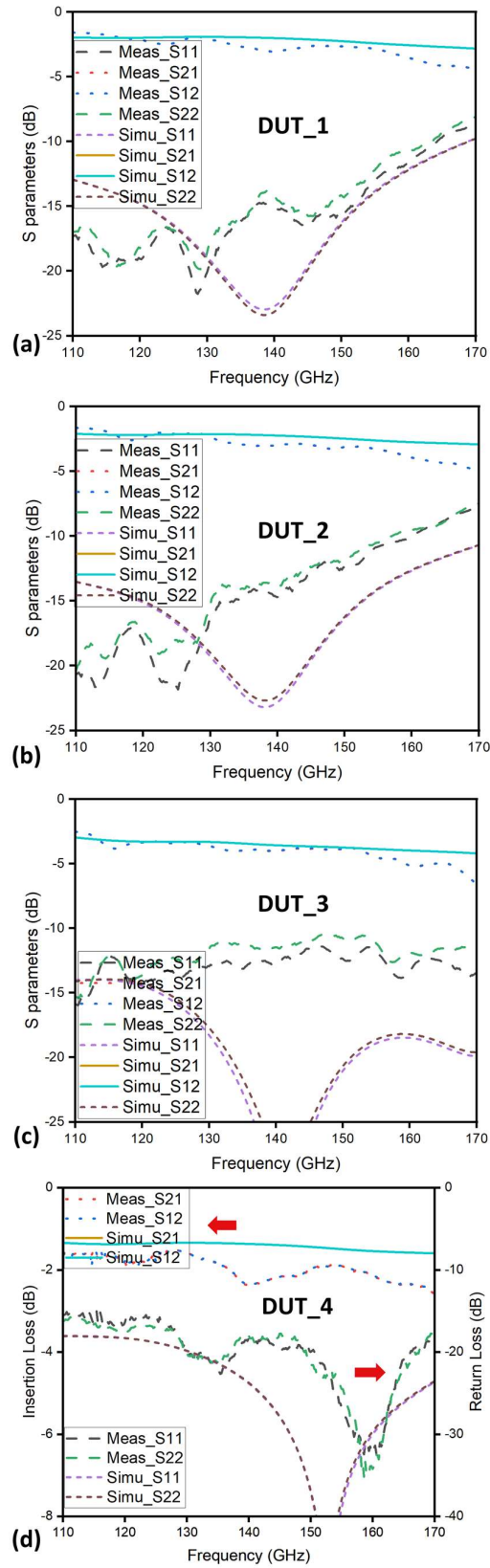


Fig. 3 The comparison between the measurement and simulation results for all four different flip-chip structures. (a), (b), (c), and (d) represent the S parameters of DUT1, 2, 3, and 4 respectively.

Table 1. The comparison of this result to the literatures

	Beer et al. [1]	Monayakul et al. [6]	Sinha et al. [7]	Khan et al. [8]	Lu et al. [9]	This work
Bumping Technology	Gold stud bump	AuSn bump	NA	Gold stud bump	Cu pillar	Cu pillar
Bump size (μm)	50	4	2	50	30	30
Insertion loss per transition	1 dB @ 170 GHz	NA	0.1 dB @ 170 GHz	0.3 dB @ 165 GHz	NA	0.3-0.5 dB @ 170 GHz
Insertion loss total structure	5.5 dB @ 170 GHz (7 mm line)	1.3 dB @ 170 GHz (0.8 mm)	1 dB @ 170 GHz (1.6 mm line)	1.2 dB @ 165 GHz (1.35 mm line)	2 dB @ 100 GHz (0.94 mm line)	2.5 dB @ 170 GHz (0.8 mm)
Transition type	CPW-CPW	STL-CPW	STL-STL	CPW-CPW	CPW-CPW	MS-MS

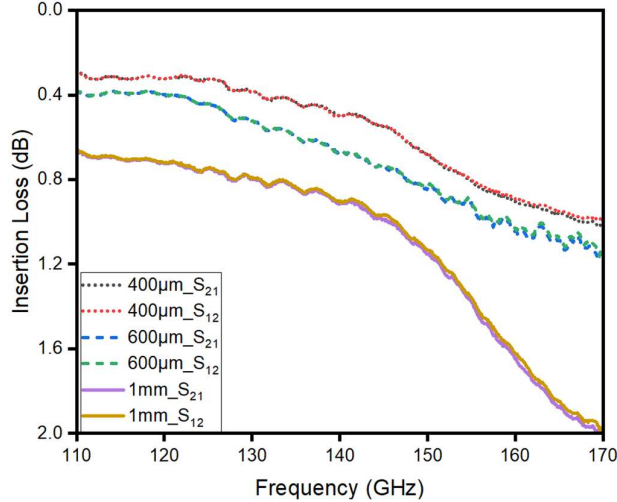


Fig. 4 The de-embedded D-band S parameter measurement of pure microstrip transmission lines with different lengths.

are achieved, validating the modelling setups. It is observed that both the pitch and the de-coupling aperture have big influences on the Cu pillar transition losses. The $|S_{21}|$ at 170 GHz corresponding to the 85 μm , 100 μm , and 150 μm pitches are -4.5 dB, -5 dB, and -6.5 dB respectively. And the DUT₄, which has an opening on the ground for de-coupling, even reduces the loss to -2.5 dB at 170 GHz. Within this context, the critical points in the transition design are the small pitch and de-coupling opening on the ground plane.

Fig. 4 shows the measurement results for the plain transmission lines after de-embedding. Considering that the total length of the flip-chip structure is 800 μm , the corresponding transmission line loss is around 1.6-2 dB at 170 GHz. The extra losses introduced by the Cu pillar transition can, therefore, be extracted by simple subtractions. A loss of 0.3-0.5 dB per Cu pillar transition over the whole D-band is obtained. A brief comparison of the flip-chip transition loss state-of-the-art is done in Table 1, where CPW stands for coplanar-waveguide, MS stands for microstrip, and STL stands for strip line. Worth noticing that Sinha et al. demonstrates a flip-chip transition only 0.1 dB loss at 170 GHz. Such a low loss is mainly attributed to two reasons: 1) an ultra-small 2 μm bump is used to minimize the parasitics, and 2) the presented D-band S-parameter measurement has huge variations (± 0.5 dB), which leads to uncertainties of the extracted per transition loss. To conclude, the extracted 0.3-0.5 dB per transition in this study agrees quite well with other results using similar sized bumps.

IV. CONCLUSION

In this paper, a Cu pillar flip-chip package is demonstrated with a loss of 0.3-0.5 dB per transition over the whole D-band.

Such a low loss agrees well with other results using similar sized bumps, indicating that the Cu pillar flip-chip can be a good alternative for D-band applications in addition to the existing technologies. The wafer-level bumping process also ensures high uniformity and throughput, making it especially suitable to be exploited for mass production of RF applications.

ACKNOWLEDGMENT

The authors would like to show the gratitude for the FLEXCOM and NANOPOLY projects, which are funded from the European Union's Horizon 2020 Programme and are under grant agreement 101004233 and 829061, respectively.

REFERENCES

- [1] S. Beer and B. Ripka and S. Diebold and H. Gulan and C. Rusch and P. Pahl and T. Zwick, "Design and measurement of matched wire bond and flip chip interconnects for D-band system-in-package applications," 2011 IEEE MTT-S International Microwave Symposium, IEEE, 2011, pp. 1-4.
- [2] P. Stärke and C. Carta and F. Ellinger, "Direct chip-to-waveguide transition realized with wire bonding for 140-220 GHz G-band", IEEE Transactions on Terahertz Science and Technology, vol. 10(3), 2020, pp. 302-308.
- [3] F. Ahmed and M. Furqan and A. Stelzer, "120-GHz and 240-GHz broadband bow-tie antennas in eWLB package for high resolution radar applications," 2018 48th European Microwave Conference (EuMC), IEEE, 2018, pp. 1109-1112.
- [4] A. Hassona and Z. S. He and V. Vassilev and C. Mariotti and S. E. Gunnarsson and F. Dielacher and H. Zirath, "Demonstration of+ 100-GHz interconnects in eWLB packaging technology," IEEE Transactions on Components, Packaging and Manufacturing Technology, vol. 9(7), 2019, pp. 1406-1414.
- [5] J. Bock and R. Lachner, "SiGe BiCMOS and eWLB packaging technologies for automotive radar solutions," 2015 IEEE MTT-S International Conference on Microwaves for Intelligent Mobility (ICMIM), IEEE, 2015, pp. 1-4.
- [6] S. Monayakul and S. Sinha and C. T. Wang and N. Weimann and F. J. Schmückle and M. Hrobak and V. Krozer and W. John and L. Weixelbaum and P. Wolter and O. Krüger, "Flip-chip interconnects for 250 GHz modules," IEEE Microwave and Wireless Components Letters, vol. 25(6), 2015, pp. 358-360.
- [7] S. Sinha and R. Doerner and F. J. Schmückle and S. Monayakul and M. Hrobak and N. G. Weimann and V. Krozer and W. Heinrich, "Flip-chip approach for 500 GHz broadband interconnects," IEEE Transactions on Microwave Theory and Techniques, vol. 65(4), 2017, pp. 1215-1225.
- [8] W. T. Khan and A. Ulusoy and R. L. Schmid and J. Papapolymerou, "Characterization of a low-loss and wide-band (DC to 170 GHz) flip-chip interconnect on an organic substrate," 2014 IEEE MTT-S International Microwave Symposium (IMS2014), IEEE, 2014, pp. 1-4.
- [9] H. C. Lu and C. C. Kuo and P. A. Lin and C. F. Tai and Y. L. Chang and Y. S. Jiang and J. H. Tsai and Y. M. Hsin and H. Wang, "Flip-chip-assembled W-band CMOS chip modules on ceramic integrated passive device with transition compensation for millimeter-wave system-in-package integration," IEEE transactions on microwave theory and techniques, vol. 60(3), 2012, 766-

